

Appendix

Table 1: Site description of all the current permanent sampling plots in the greater Yangambi region. We list the forest type, plot number, geographic location (in decimal degrees), stem density, basal area Above Ground Carbon (AGC), species richness and Land-Use and Land-Cover Change (LULCC) classes in a radius of 100m around each plot location.

type	nr	latitude	longitude	stem density (ha^{-1})	basal area ($m^2 ha^{-1}$)	AGC (Mg C ha^{-1})	species richness	LULCC class coverage (%)
fallow	1	0.7959139	24.49423	350	5.39000	6.7000	26	37 (1), 63 (3)
fallow	2	0.7921028	24.49717	132	2.06000	2.0400	22	68 (1), 32 (3)
young-regrowth	1	0.7894028	24.51755	322	20.44000	46.5600	40	68 (1), 32 (3)
young-regrowth	2	0.7948806	24.49193	447	16.63000	27.8300	25	56 (1), 44 (3)
young-regrowth	3	0.7931083	24.49013	313	17.80000	37.1000	43	51 (1), 49 (3)
old-regrowth	1	0.8824444	24.49614	384	19.48000	81.7800	92	100 (1)
mixed	1	0.8135486	24.51264	563	34.81000	168.0400	83	100 (1)
mixed	2	0.7805000	24.52109	403	35.25000	174.5800	78	100 (1)
mixed	3	0.7866181	24.52349	367	30.69000	150.3000	75	100 (1)
mixed	4	0.8140333	24.49370	432	33.01000	168.6100	84	100 (1)
mixed	5	0.8025611	24.48750	329	25.20000	124.1800	80	100 (1)
mixed	6	0.9925556	24.53906	490	32.63000	203.8100	86	100 (1)
mixed	7	0.9898056	24.53853	598	31.47000	146.1100	92	100 (1)
mixed	8	0.9866111	24.53856	556	29.20000	148.2100	90	100 (1)
mono-dominant	1	0.8269306	24.52303	344	31.80000	183.0100	48	100 (1)
mono-dominant	2	0.8282708	24.53196	436	32.06000	173.5800	55	100 (1)
mono-dominant	3	0.7965903	24.49779	376	30.57000	166.4400	62	100 (1)
mono-dominant	4	0.8080889	24.52811	374	27.69000	145.5500	46	100 (1)
mono-dominant	5	0.8682806	24.45655	217	27.19000	159.0000	46	95 (1), 5 (2)
mono-dominant	6	0.7992278	24.49195	378	33.95000	165.4800	68	100 (1)
edge	1	0.7895486	24.51990	415	30.93601	152.2792	77	100 (1)
edge	2	0.7979472	24.48885	368	31.82097	152.1736	72	95 (1), 5 (3)
edge	3	0.8144250	24.48555	458	35.79959	197.4022	86	100 (1)
edge	4	0.7659306	24.51125	320	29.72547	154.6380	75	98 (1), 2 (3)
edge	5	0.8691778	24.47019	459	33.72462	158.6934	88	100 (1)

Table 2: Flight path meta-data for the Isangi-Stanleyville aerial survey. Data provided consists of the flight path number, cardinal direction of the flight, the image numbers, and the duration of the flight provided by the start and end time of the acquisition. Data is sourced from Appendix Figure 2 and the sensor logs recorded in the margin of acquired images (see Figure 1 main manuscript).

path	direction	image #	start (H:M:S)	end (H:M:S)
1	W – E	04 / 78 – 04 / 127	10:15:00	10:40:00
2	W – E	05 / 01 – 05 / 56	10:15:00	10:40:00
3	W – E	06 / 01 – 06 / 48	08:55:00	09:20:00
4	W – E	07 / 01 – 07 / 20	09:30:00	09:45:00
5	W – E	05 / 167 – 05 / 187	08:55:00	09:10:00
6	W – E	07 / 67 – 07 / 82	10:50:00	11:00:00
7	E – W	06 / 49 – 06 / 95	09:35:00	10:05:00
8	E – W	05 / 57 – 05 / 103	10:20:00	10:50:00
9	E – W	04 / 128 – 04 / 176	10:50:00	11:10:00
10	W – E	08 / 01 – 08 / 27	09:05:00	09:20:00
11	W – E	06 / 96 – 06 / 139	10:25:00	10:45:00

\begin{table}[!h]

\caption{Contingency table in agreement (%) between forest / non-forest classes as generated from a Geo-Eye 1 pan-chromatic image using a Convolutional Neural Network (CNN) generated and the Global Forest Cover map (Hansen et al. 2013).}

CNN	Global Forest Cover	
	non-forest	forest
non-forest	10	9
forest	4	77

\end{table}

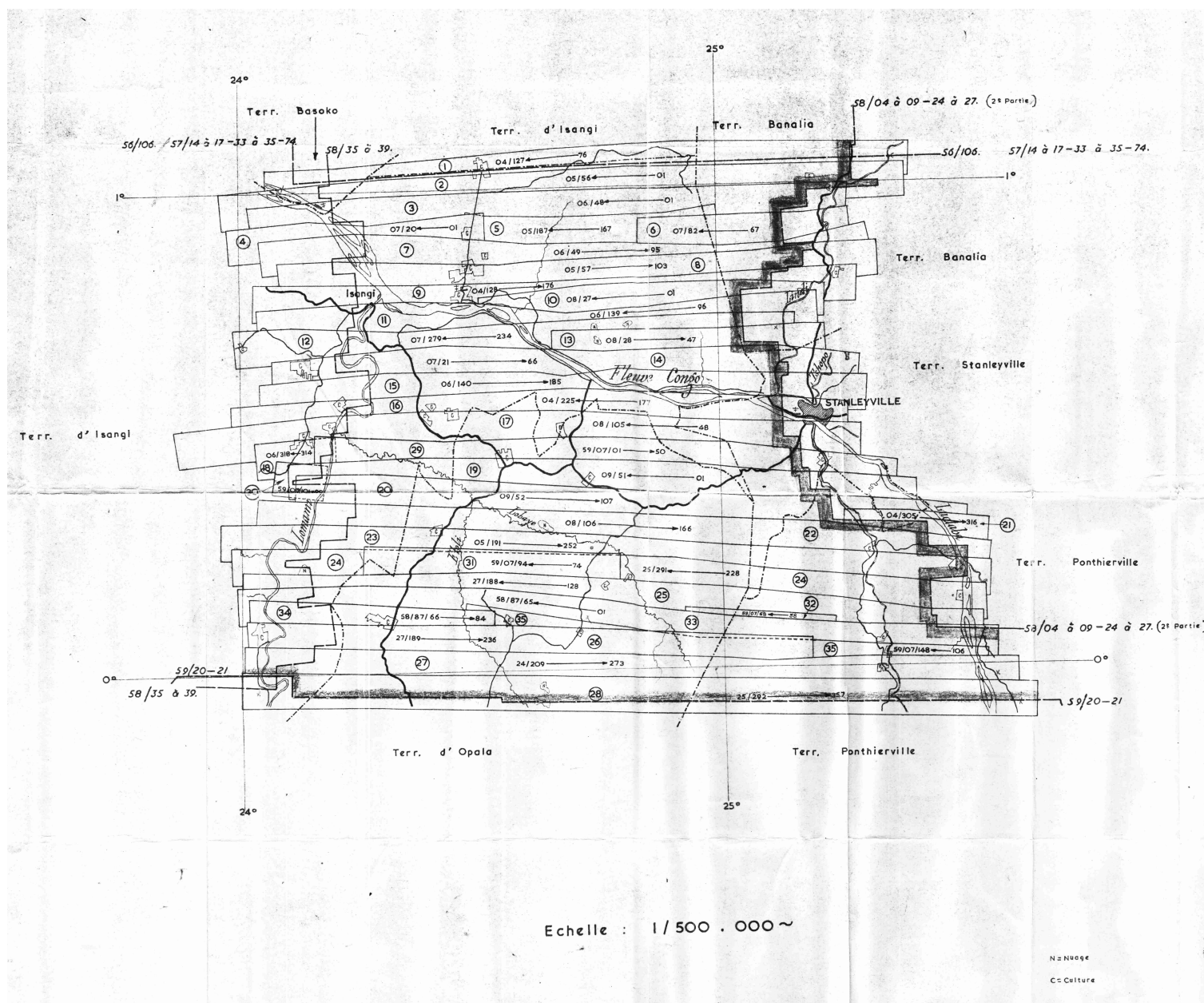


Figure 1: Overview of the complete flight plan of the survey around Kisangani (then Stanleyville) stored in the archives at the Africa Museum.

ISANGI — STANLEYVILLE (1^{re} Partie) 59/07

58/04-05-06-07-08-09-24-25-27-87.

Date de prises de vues : 6/1/58 au 20/2/58. 26/2/58 au 9/1/59.
Appareil de prises de vues : Camera Wild FCSa - L404 Avigon

Distance focale : 114,83 mm

Altitude objective : 5.200 m

Altitude de survol : 4.600 m.

Altitude approximative au sol : 600 m

Echelle approximative : 1/40.000

Surface couverte : 18.530 Km²

Bandes	Couverture utile	Genres	Double emploi	à rejeter	Double emploi Couverture plus récente
1 [X 1 X 2	58/04/78 à 127 " 05/01 " 56	Inf. rouge			76 et 77
2 [X 3 X 4 X 5	" 06/01 " 48 " 07/01 " 20 " 08/07 " 187	"	156 à 166 et 188 à 190		67 " 68 93 " 95
3 [X 6 X 7	" 07/69 " 82 " 08/42 " 92	"			101 " 103 174 " 176 01 " 02 96 " 98
4 [X 9 X 10 X 11	" 05/57 " 100 " 04/128 " 173 " 08/03 " 27	"			46 " 47 64 " 66 181 " 185 177 " 178 48 " 49 270 " 313 01 " 05 98 " 107 314 " 316
5 [X 12 X 13 X 14	" 06/199 " 139 " 07/234 " 279 " 08/28 " 45 " 07/21 " 63	"	58/07/280 à 323 Couvert par bande 20/1423		
6 [X 15 X 16	" 06/140 " 180 " 04/179 " 225	"			
7 [X 17 X 18	" 08/50 " 105 " 06/314 " 318	"			
8 [X 19 X 20	" 09/06 " 51 " 09/52 " 97	"			
9 [X 21 X 22	" 04/305 " 313 " 08/106 " 166	"			
10 [X 23 X 24	" 05/191 " 252 " 25/230 à 299 et 291	"		260 à 279	228 " 229
11 [X 25 X 26	" 27/128 " 188 " 27/180 " 223	"			224 " 236
12 [X 27 X 28	" 24/209 " 273 " 25/292 " 357	"			
13 [X 29 X 30 X 31	58/07/01 " 50 " 27/99 " 101 " 07/74 " 94	"	95 à 98 et 102 à 105		
14 [X 32 X 33 X 34	" 07/58 " 68 58/87/01 " 65 " 87/66 " 84	"	91 à 97 et 99 à 73		
15 [X 35	59/07/106 " 148	"	85 " 92		

Figure 2: Overview of the complete flight plan meta-data as stored in the archives at the Africa Museum.

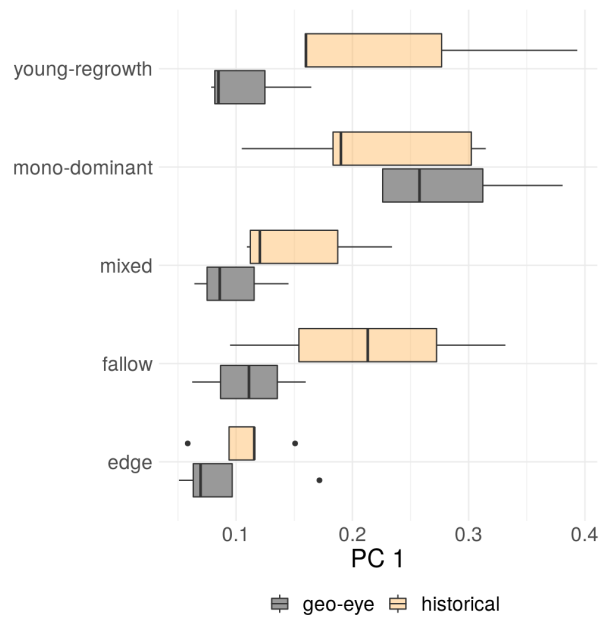


Figure 3: Boxplots comparing the first principal component (PC1) of a site based FOTO analysis across different forest types for both contemporary (Geo-Eye) and historical orthomosaic data.

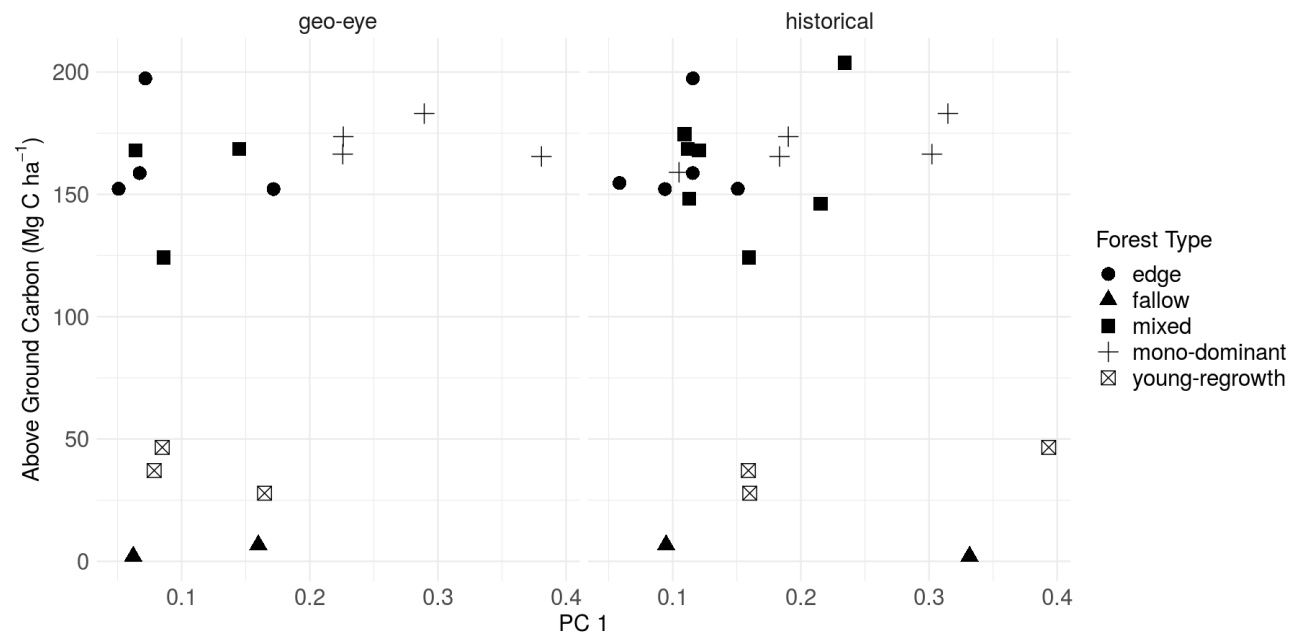


Figure 4: Scatterplot comparing Above Ground Carbon and the first principal component of the FOTO analysis for contemporary Geo-Eye (left) and the historical orthomosaic (right) data. Different forest types are plotted using closed circles, closed triangles, closed squares and this for fallow, mixed mono-dominant and young-regrowth forests, respectively

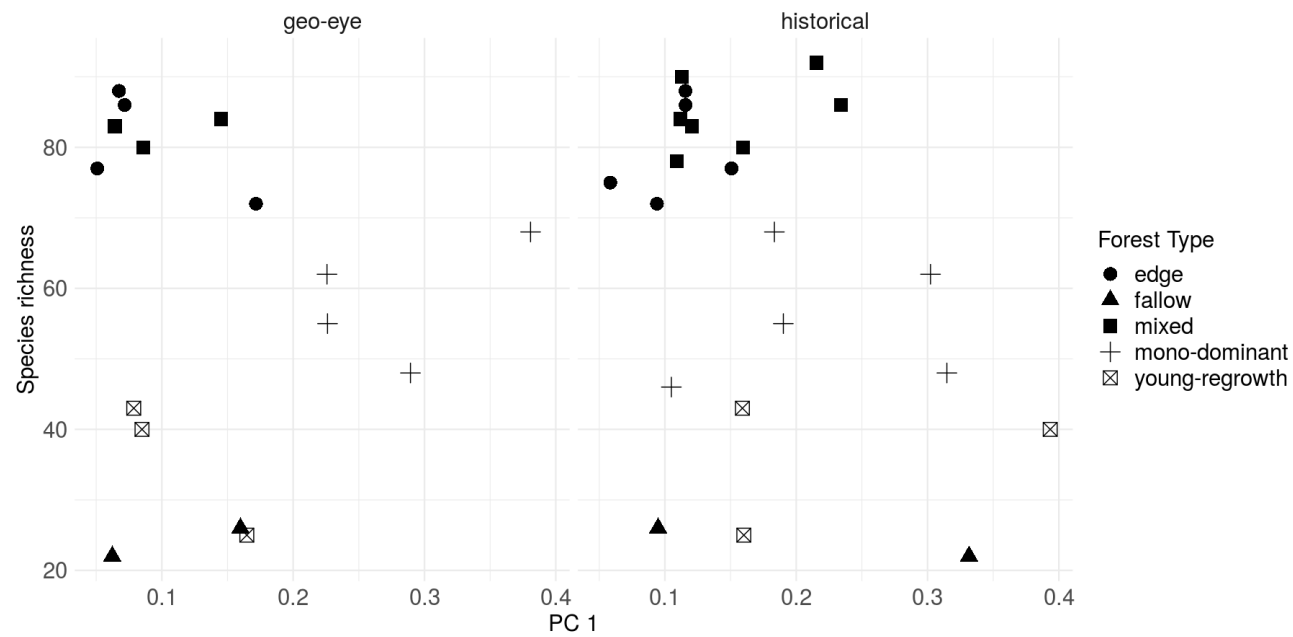


Figure 5: Scatterplot comparing tree species richness and the first principal component of the FOTO analysis for contemporary Geo-Eye (left) and the historical orthomosaic (right) data. Different forest types are plotted using closed circles, closed triangles, closed squares and this for fallow, mixed mono-dominant and young-regrowth forests, respectively

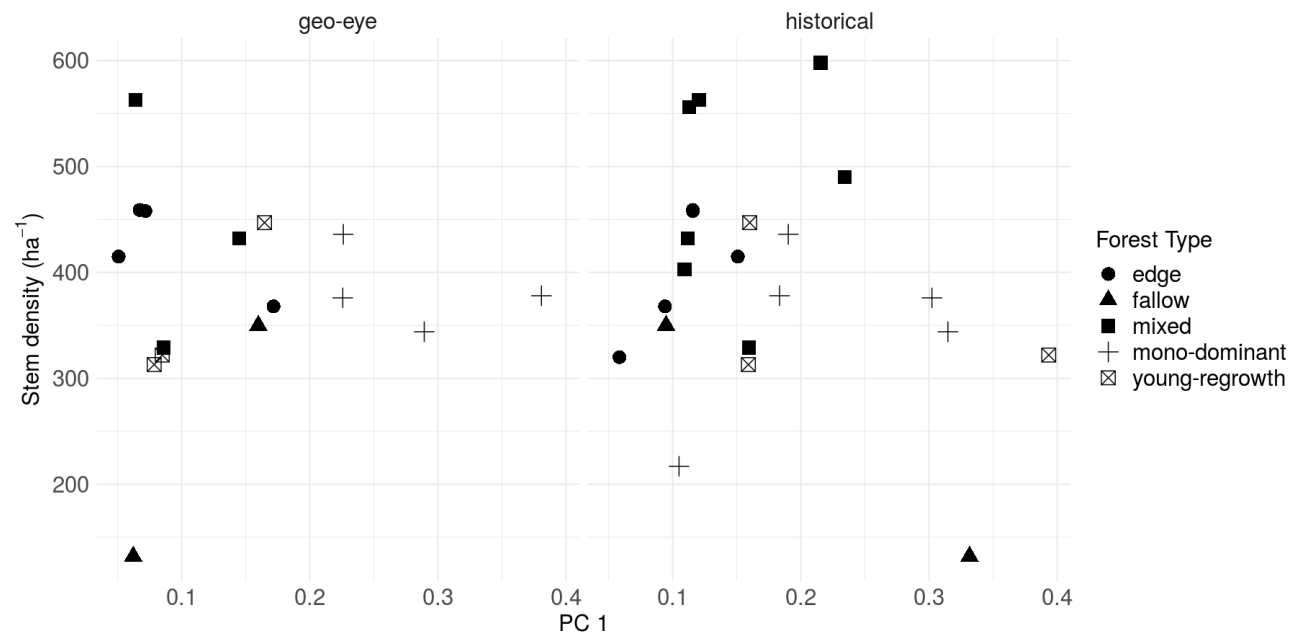


Figure 6: Scatterplot comparing stem density (per ha) and the first principal component of the FOTO analysis for contemporary Geo-Eye (left) and the historical orthomosaic (right) data. Different forest types are plotted using closed circles, closed triangles, closed squares and this for fallow, mixed mono-dominant and young-regrowth forests, respectively

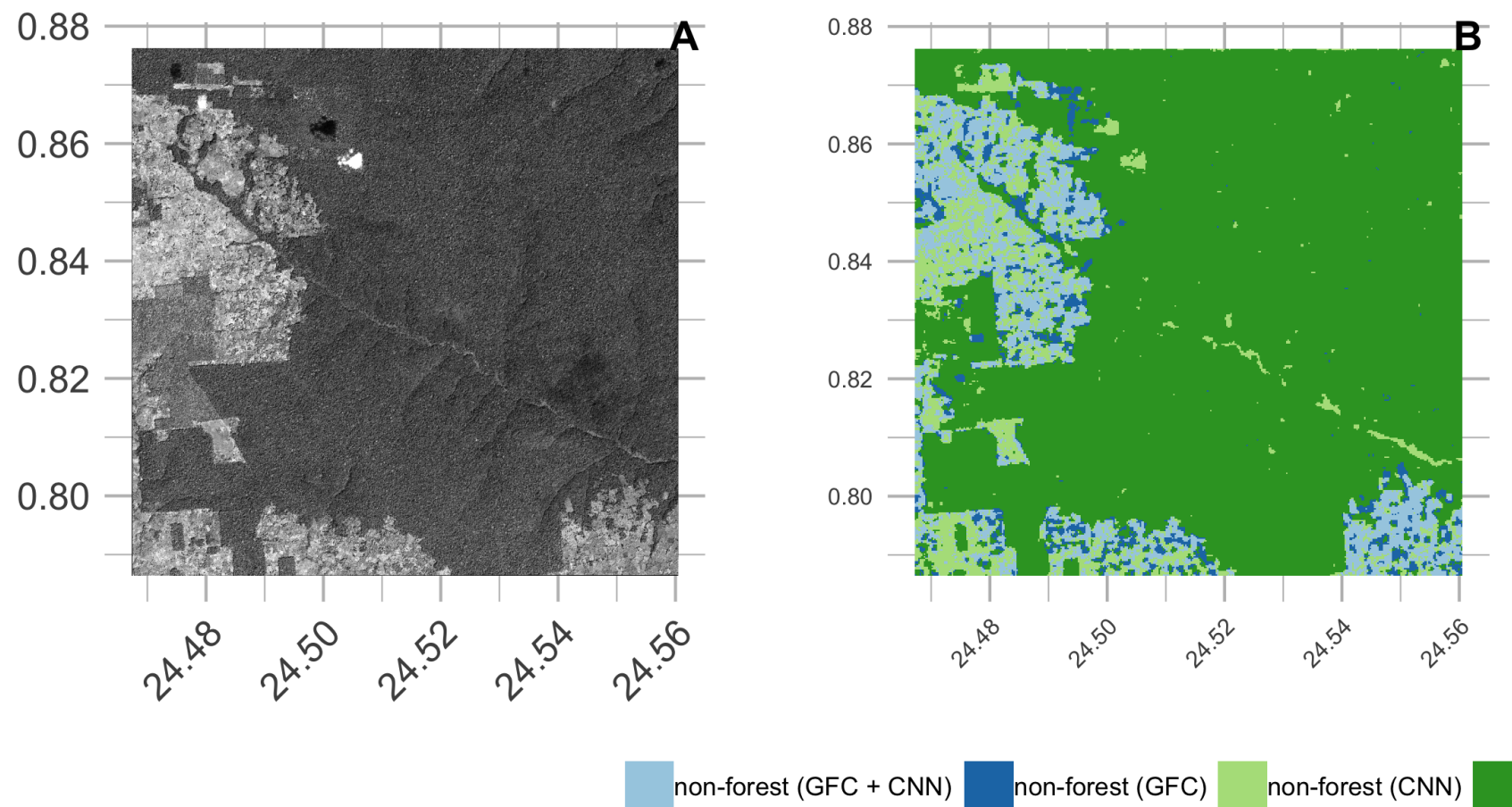


Figure 7: CNN classifier results as run on a recent (2012) Geo-Eye panchromatic image. Results are compared with the Landsat based .